

## Alteration of first-order phase transition by stress cycles in a MnAs layer on step-bunched GaAs(331)B

Y. Takagaki, C. Herrmann, B. Jenichen, and J. Herfort

*Paul-Drude-Institut für Festkörperelektronik, Hausvogteiplatz 5-7, 10117 Berlin, Germany*

(Received 9 February 2009; revised manuscript received 24 April 2009; published 18 June 2009)

We demonstrate a manipulation of the first-order phase transition in a MnAs layer grown on step-bunched GaAs(331)B. The layer is composed of alternating (1 $\bar{1}00$ )- and (11 $\bar{2}2$ )-oriented segments, which grew on (110) terraces and sidewalls consisting of bunched steps, respectively. The shape of the thermal hysteresis curves in magnetization and resistance changes markedly with temperature cycles. The alteration is associated with improvements in the crystalline quality. Out-of-plane components of the phase-transition stress resulting from the nonplanar geometry of the layer are indicated to be the driving force for the annealinglike elimination of structural imperfections. Plastic flow of materials induced by the stress is evidenced to almost completely level the surface height modulations having an amplitude of about 50 nm.

DOI: [10.1103/PhysRevB.79.235320](https://doi.org/10.1103/PhysRevB.79.235320)

PACS number(s): 64.60.Ej, 61.72.Hh

### I. INTRODUCTION

Bulk MnAs undergoes simultaneous magnetic and structural phase transitions at Curie temperature  $T_C \approx 315$  K.<sup>1,2</sup> The phase transition is of first order. A first-order phase transition does not occur immediately but is initiated by nucleation. When the temperature crosses  $T_C$ , the system stays in a metastable state until nuclei are formed by surmounting a potential barrier separating the phases. The nuclei are favored and thus grow further until a macroscopic phase transition has been accomplished. The phase transition is, therefore, characteristically accompanied by a thermal hysteresis.

The microscopic mechanism of the phase transition in MnAs is not fully understood despite numerous investigations over half a century. Specifically, the magnetic state in the phase above  $T_C$  ( $\beta$ -MnAs) remains controversial.<sup>3,4</sup> The magnetic order in  $\beta$ -MnAs is generally considered to be paramagnetic as neutron-scattering measurements have found no evidence for a long-range magnetic order.<sup>5</sup> However, the characteristics of  $\beta$ -MnAs rather make sense if the magnetic order is antiferromagnetic.<sup>6-8</sup>

The ferromagnetic phase of MnAs ( $\alpha$ -MnAs) possesses a hexagonal crystal structure.<sup>9</sup> MnAs is attractive for spintronics applications as, in addition to  $T_C$  being above room temperature, epitaxial growth on GaAs and Si is possible.<sup>10,11</sup> In the emerging field of spintronics, the transport of spin rather than charge is utilized for the purpose of information processing. Creating and detecting spin polarization are crucial operations in the spin manipulation, for which ferromagnet/semiconductor heterojunctions are naturally an essential element. Spin injection from a MnAs layer to a GaAs-(In,Ga)As quantum well<sup>12</sup> and spin accumulation at a MnAs-GaAs interface<sup>13</sup> have already been demonstrated. The material properties of epitaxial layers are often affected by the inevitable existence of the substrates. The MnAs/GaAs system is a typical example of such, where the structural, magnetic, and electrical properties in MnAs layers have been revealed to be modified by the stress imposed by the substrates.<sup>11,14</sup> There is hence prospect of, for instance, increasing spin polarization at the Fermi level<sup>15</sup> as well as  $T_C$  by optimization of the influence of the substrate.

In the present paper, we report a dramatic influence of the substrate on the first-order phase transition. The phase transition and thermal hysteresis in MnAs layers grown on GaAs(331)B are shown to behave in a peculiar manner. The magnetization and resistance of the as-grown MnAs layers exhibit a permanent alteration of the thermal hysteresis curves with thermal cycles. The potential barrier for the phase transition is thus manifested to be varied through the crystalline structure of the epitaxial layers.

### II. GROWTH

The growth of the MnAs/GaAs(331)B heterostructure was carried out in a molecular-beam epitaxy (MBE) chamber. The initial GaAs buffer layer was grown on an “epiready” substrate by migration-enhanced epitaxy with a thickness of 10 nm. The substrate temperature was  $T_s = 520$  °C. The As<sub>4</sub>/Ga beam-equivalent pressure (BEP) ratio was 26. Following an annealing at 600 °C for 1 min, a 180-nm-thick GaAs layer was further grown by conventional MBE at  $T_s = 520$  °C with a BEP ratio of 44. The growth rate was 3.1 nm/min. The buffer layer was again annealed at 600 °C for 1 min.

The preparation of the GaAs buffer layer was followed by the growth of a MnAs layer using a procedure based on solid phase epitaxy (SPE).<sup>16</sup> An amorphous MnAs layer was deposited at  $T_s = 200$  °C with an As<sub>4</sub>/Mn BEP ratio of 380. It is crucial for the SPE-based procedure that the thickness of the amorphous layer, 2 nm, is larger than the critical thickness for coherent growth, which is less than 1 nm.<sup>17,18</sup> The disappearance of the reflection high-energy electron diffraction (RHEED) pattern from the GaAs buffer layer was utilized to make certain of a complete coverage of the surface by the amorphous layer. The amorphous layer was then crystallized by increasing  $T_s$  to 250 °C in an arsenic-free environment. The thus-prepared layer was used as a growth template to obtain a MnAs layer having a thickness of 125 nm by a conventional MBE growth. The BEP ratio and the growth rate in the conventional growth were 28 and 2.6 nm/min, respectively.

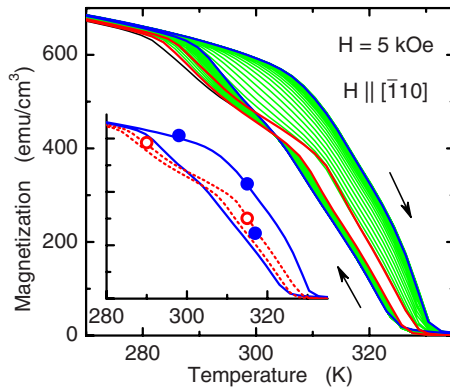


FIG. 1. (Color online) Temperature dependence of magnetization of a MnAs layer on GaAs(331)B measured using a SQUID magnetometer. An as-grown layer was subjected to 22 thermal cycles. Temperature was swept at a rate of 1.5 K/min. An in-plane external magnetic field  $H=5$  kOe was applied along the GaAs $[\bar{1}10]$  direction, which is parallel to the magnetic easy axis. The arrows indicate the direction of the temperature sweeps. The initial and final curves are shown in the inset by the dotted and solid lines, respectively. The measurements in Fig. 7 were performed at the conditions indicated by the circles. The open and filled circles correspond to the initial and final states, respectively.

### III. RESULTS

We have examined the thermal hysteresis in magnetization and resistance of the MnAs layer. In Fig. 1, we show the dependence of magnetization measured using a superconducting quantum interference device (SQUID) magnetometer on temperature  $T$ . In order to align the magnetization, an in-plane external magnetic field  $H(=5$  kOe) was applied in the direction of the magnetic easy axis, which is parallel to the GaAs $[\bar{1}10]$  direction. The temperature dependence in the range plotted in Fig. 1 is governed by the coexistence of  $\alpha$ - and  $\beta$ -MnAs.<sup>19</sup> The phase transition of MnAs at  $T_C$  involves a discontinuous lattice-constant change in the  $a$ -axis direction.<sup>20</sup> The lattice constant changes in a way to be able to cancel the thermal stress and so the  $\alpha$  and  $\beta$  phases coexist in epitaxial layers over a certain temperature interval in order to reduce the strain energy. One can directly see the phase coexistence in the scanning electron micrograph in Fig. 2(a) as the stripe pattern repeated in the GaAs $[\bar{1}10]$  direction. The phase fraction and thus the magnetization changes approximately linearly with temperature in the coexistence range.

As evident in Fig. 1, the hysteresis loop changes remarkably with temperature cycles around the phase-transition region. (The measurements were performed over 22 thermal cycles using a temperature sweep rate of 1.5 K/min.) The hysteresis loop is found to shift gradually to high temperatures. In particular, the onset of the creation of the  $\beta$  phase in the temperature sweep up appears to increase from 285 to  $\sim 305$  K. The permanent alteration of the thermal hysteresis was observed also for the resistance, as shown in Fig. 3. (The temperature sweep rate in this set of measurements was not constant.) The hysteresis loops in magnetization and resistance are seen to change in the same manner wherever comparison is possible.

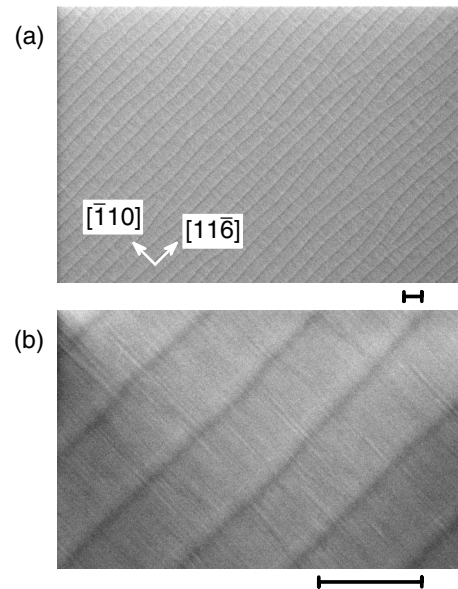


FIG. 2. Scanning-electron micrographs of a MnAs layer on GaAs(331)B at room temperature. The  $[\bar{1}10]$  and  $[11\bar{6}]$  directions of the substrate are indicated. The scale bars show the length of 1  $\mu\text{m}$ .

The peculiar behavior of the thermal hysteresis is attributed to an unusual topography of the MnAs layer. In Fig. 4, we show three x-ray diffraction (XRD) curves taken from the MnAs layer. The middle curve was obtained under the ordinary measurement configuration. No peak associated with the MnAs layer was found, except for the two small peaks shown in the inset with expanded scales. However, strong peaks emerged when the specimen was rotated around the  $[\bar{1}10]$  axis of the substrate. For the top and bottom curves, the rotation angles are  $-6.2^\circ$  and  $12^\circ$ , respectively. This dependence on the angle of incidence originates from the step bunching that occurred during the growth of the GaAs buffer layer.<sup>21</sup> The (331) surface of GaAs developed into terraces and sidewalls consisting of bunched steps. (1 $\bar{1}00$ )- and

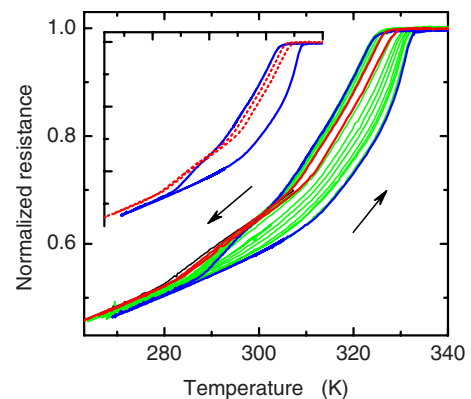


FIG. 3. (Color online) Temperature dependence of resistance of a MnAs layer on GaAs(331)B. The arrows indicate the direction of the temperature sweeps. Temperature was not swept at a constant rate. The initial and final curves are shown in the inset by the dotted and solid lines, respectively.

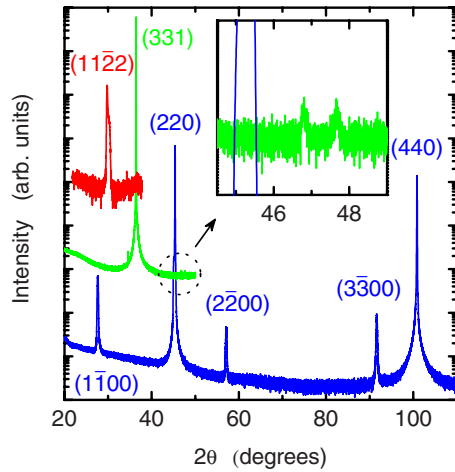


FIG. 4. (Color online) X-ray diffraction curves ( $\omega$ - $2\theta$  scan) obtained from a MnAs layer on GaAs(331)B. The peaks denoted with three and four indices are associated with the substrate and overlayer, respectively. The middle curve was measured with the ordinary sample configuration. For the top and bottom curves, the specimen was tilted around the  $[\bar{1}10]$  axis of the substrate by  $-6.2^\circ$  and  $12^\circ$ , respectively. The curves are offset for clarity. The region encircled by the dotted line is shown with expanded scales in the inset.

$(11\bar{2}2)$ -oriented MnAs layers grew on the respective regions, as illustrated in Fig. 5. The step bunching is visible in Fig. 2(b) as a weak streaky feature orthogonal to the  $\alpha$ - $\beta$  stripes. We also show an atomic force micrograph in Fig. 6(a). The line scan in Fig. 6(b) shows that the surface modulation produced by the step bunching retains a typical period of about 40 nm and an amplitude of about 10 nm after an overgrowth of the MnAs layer.

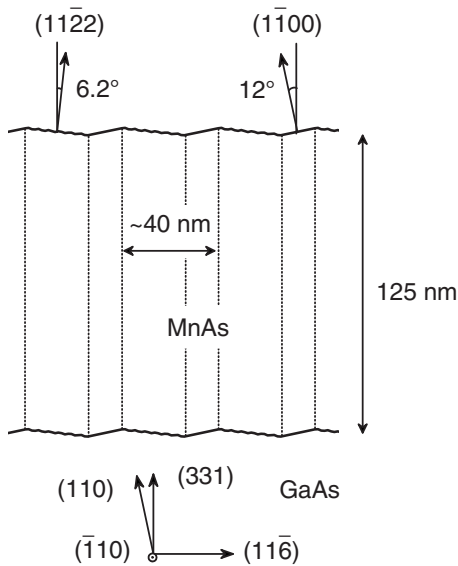


FIG. 5. Schematic of a MnAs layer grown on a step-bunched GaAs(331)B substrate. Here, the step bunching is assumed to form the simplest structure by regularly alternating two components. The terraces of the (110) facet of GaAs and the sidewalls consisting of bunched steps are inclined by 12 and  $6.2^\circ$ , respectively. The MnAs segments on respective regions are  $(11\bar{0}0)$  and  $(11\bar{2}2)$  oriented.

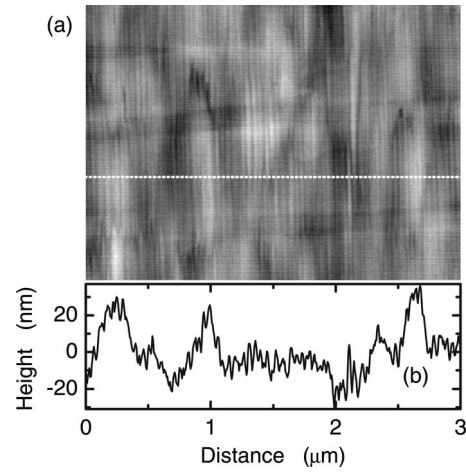


FIG. 6. (a) Atomic force micrograph of an as-grown MnAs layer on GaAs(331)B. The  $[\bar{1}10]$  and  $[11\bar{6}]$  directions of the substrate are aligned in the vertical and horizontal directions, respectively. The sizes of the scan area are  $3.0 \times 2.2 \mu\text{m}^2$ . (b) Line scan at the position indicated by the dotted line in (a).

When the rotation angle was adjusted around  $12^\circ$  to maximize the diffraction intensity from the MnAs layer, peaks associated with the (220) and (440) diffractions from the substrate appeared (bottom curve in Fig. 4). This indicates that the terraces in the step bunching are formed by (110) facets. To our knowledge, the surface orientation of the terraces of the step bunching has not been clearly identified. The heteroepitaxy of a highly dissimilar layer has enabled the unambiguous determination of the terrace orientation. We note that not only the inclination angle of the (110) facet ( $12^\circ$ ) but also that of the bunched steps ( $-6.2^\circ$ ) correspond well to the transmission electron micrograph of step bunching presented in Ref. 22.

The clear stripe pattern resulting from the phase coexistence in Fig. 2 manifests a good crystalline homogeneity in the MnAs layer. The excellent quality of the MnAs layer is also evidenced by the presence of higher-order diffraction peaks in the bottom curve in Fig. 4. The crystal quality of MnAs layers on GaAs(110) prepared by means of SPE is better than that of layers grown by conventional MBE.<sup>16</sup> The epitaxial orientation relationship in SPE is overwhelmingly determined by the strain energy.<sup>23</sup> If the mismatch in the lattice constants between the layer and the substrate is large, the lack of optimum crystal orientation leads to a mixture of various surface orientations and in-plane tilts in the layers. In contrast, the inflexibility of the growth mode acts to suppress the orientational spread when the mismatch is small, which is the case for the (110)-oriented substrate.

Nonetheless, the well-developed  $\alpha$ - $\beta$  stripe pattern in Fig. 2 is surprising as it is unexpected for the  $(11\bar{2}2)$ -oriented component of the MnAs layer for two reasons. (i) The stripe pattern is a characteristic feature when the  $c$  axis of MnAs lies in the surface plane. The large tilt of the  $c$  axis to the out-of-plane direction ( $33^\circ$ ) is thus unfavorable for the  $\alpha$ - $\beta$  stripe. The phase coexistence in (0001)-oriented MnAs layers takes place in the form of islands of  $\alpha$ -MnAs interwoven in a honeycomblike network of  $\beta$ -MnAs.<sup>24</sup> (ii) The compo-

ment grew on the bunched steps, i.e., on unspecific surface orientations. One would rather anticipate a poor crystal quality and nonrigorous epitaxial alignments for such a circumstance. Moreover, the fraction of the  $(11\bar{2}2)$ -oriented component is estimated to be 66% from the tilt angles. Instead of the  $(1\bar{1}00)$ -oriented component on the  $(110)$  terraces that could account for the clear  $\alpha$ - $\beta$  stripe, the  $(11\bar{2}2)$ -oriented component would be the dominant one in establishing the distribution pattern of the two phases. At present, the reason for the seeming dominance of the  $(1\bar{1}00)$ -oriented component is not understood.

#### IV. DISCUSSION

The alteration of the hysteresis loops was observed to be insensitive to the maximum and minimum temperatures of the sweeps as long as the temperature was varied over a range wider than that of the phase coexistence. The modification is hence suggested to be caused by the phase-transition stress rather than a thermal effect. In polycrystalline bulk MnAs, the resistance was reported to increase as temperature crosses  $T_C$  due to the generation of microcracks by the phase-transition stress.<sup>25,26</sup> On the contrary, the resistance decreases with thermal cycles in Fig. 3, indicating an improvement in the material properties as if the sample were annealed. As demonstrated in Ref. 14, the residual resistivity in MnAs layers grown on various substrate orientations spreads over, at least, 2 orders of magnitude, reflecting the various degrees of scattering of conduction carriers from the structural and magnetic domains. The residual resistivity in the layer on GaAs(331) $B$  is only several times larger in comparison to the cases of the lowest resistivity.<sup>14</sup> Because of the relatively good crystalline order in the as-grown layer, the resistance decrease in Fig. 3 is merely several percent. Consequently, no change that collaborates with improvements in the material quality was detected by XRD as its sensitivity is not as good as the resistance measurements.

We speculate that the improvement of the crystallinity in the layer was driven by the phase-transition stress. The remarkable modification of the hysteresis occurs only in layers grown on GaAs(331) $B$ .<sup>14</sup> The unusual topography of the layer due to the step bunching apparently plays an important role. That is, the MnAs layer is zigzag shaped rather than being planar. This yields a unique distribution of stress that contains out-of-plane components. The twist of the layer by thermal cycles is suggested to enhance the migration of defects and impurities to strain “focal points,” which is likely to be located at the boundaries between the  $(1\bar{1}00)$ - and  $(11\bar{2}2)$ -oriented components, i.e., above the ridges and grooves of the step bunching (see Fig. 5).

The expansion of the hysteresis loops after thermal cycles in Figs. 1 and 3 implies an increase in the potential barrier for the first-order phase transition. The increase is ascribed to the reduction in the number of nucleation centers that trigger the phase transition as a consequence of the presumed removal (or relocation) of crystalline imperfections. It is intriguing that the change is significant for the nucleation of the  $\alpha$  phase in temperature sweep up while the nucleation of

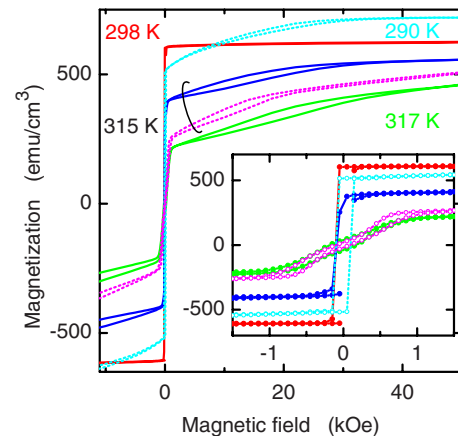


FIG. 7. (Color online) Dependence of magnetization on an in-plane external magnetic field  $H$  applied along the magnetic easy axis, which is parallel to the GaAs $[\bar{1}10]$  direction. The measurements were carried out for  $|H| \leq 50$  kOe at the denoted temperatures, which are also indicated by the circles in the inset of Fig. 1. The dotted and solid lines correspond to the initial and final states of the hysteresis loop, respectively. The diamagnetic contribution of the GaAs substrate has been subtracted. The inset shows the magnetic hysteresis loops in the low-field region.

the  $\beta$  phase in temperature sweep down is hardly affected. The relocation of defects and impurities driven by the phase-transition stress can affect the magnetoelastic effects. Local modifications in the stress distribution may account for the stabilization of the  $\alpha$  phase after thermal cycles through the magnetoelastic effects. We note in this respect that hydrostatic pressure is known to lower  $T_C$  in bulk MnAs.<sup>2</sup>

A comparison between the MnAs layers grown on various surface orientations of the substrates has revealed that the most pronounced temperature hysteresis is obtained for MnAs layers having the highest crystalline order.<sup>14</sup> Although this is what is expected for a first-order phase transition in bulk materials, as we mentioned above, the opposite is, in fact, anticipated in epitaxial layers. In the phase-coexistence regime, the domains of  $\alpha$ - and  $\beta$ -MnAs are already present. The change in the phase fractions when temperature is varied can progress as growth and annihilation of the existing domains. As the potential barrier for such a movement of the domain boundaries is zero, the temperature dependencies of magnetization and resistance would exhibit no hysteresis. A hysteresis emerges when the domain boundary movement is hindered by the pinning at crystalline imperfections, i.e., broader hysteresis loops are associated with poorer material qualities. The experimental results seem to suggest that the phase fractions vary in the present layer through nucleations in the phase domains rather than domain-boundary movements.

There is another characteristic in the alteration of the hysteresis loops that is attributed to the reduction in disorder. The initial magnetization and resistance curves exhibit a change in the slope at about 310 K. As shown in the inset of Fig. 7, the dependence of magnetization on  $H$  changes between the abrupt flipping at coercive fields ( $\sim 100$  Oe) for the low-temperature side and the gradual tilting for the high-temperature side. The transition between the easy- and hard-

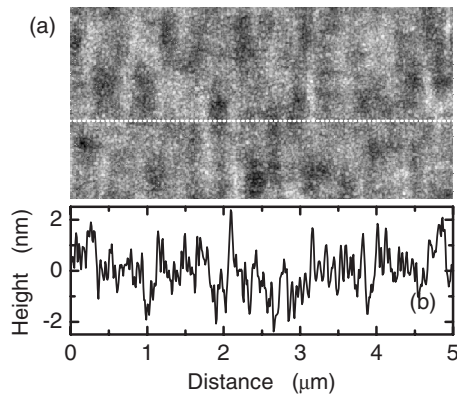


FIG. 8. (a) Atomic force micrograph of a MnAs layer on GaAs(331) $B$  after thermal cycles. The  $[\bar{1}10]$  and  $[11\bar{6}]$  directions of the substrate are aligned in the vertical and horizontal directions, respectively. The sizes of the scan area are  $5.0 \times 2.5 \mu\text{m}^2$ . (b) Line scan at the position indicated by the dotted line in (a).

axis behaviors is understood in terms of a breakup of the strips of  $\alpha$ -MnAs in the  $\alpha$ - $\beta$  stripe into small islands due to disorder.<sup>14,27</sup> The shape anisotropy reorients the magnetic easy axis to the out-of-plane direction if the lateral size of the islands is smaller than the layer thickness. The shoulder in the temperature dependence becomes nearly unrecognizable after thermal cycles. This suggests that continuous strips of  $\alpha$ -MnAs are maintained nearly until the disappearance of the  $\alpha$  phase owing to the weakened disorder.

Even when the magnetic hysteresis exhibits rectangular switching profile at weak fields, magnetization generally increases gradually with the external magnetic field in the high-field region as shown in Fig. 7. Such a behavior occurs as the field cannot be exactly aligned along the magnetic easy axis because of the zigzag shape of the MnAs layer. However, in the curve measured at  $T=298$  K for the final state after thermal cycles, magnetization almost saturates with a flipping at the coercive field. This may be interpreted to mean that the zigzag shape of the MnAs layer is flattened by the stress cycles. Indeed, as shown by the atomic force micrograph in Fig. 8, the height modulation in the surface is found to be drastically leveled after thermal cycles. [The streaky feature of the step bunching remained visible in scanning electron microscopy even after the thermal cycles (not

shown).] The primary phase-transition stress is in the  $[\bar{1}10]$  direction of the substrate. In a planar layer, the secondary stress in the orthogonal direction in the surface plane due to the Poisson effect is zero because of the translational symmetry. However, the stress in the  $[11\bar{6}]$  direction of the substrate is generated in the MnAs/GaAs(331) $B$  system as the zigzag geometry of the MnAs layer breaks the translational invariance. This stress is seen to be strong enough to cause the plastic flow of materials. The flow is anticipated to induce segregation of dislocations to the surface, thereby giving rise to the decrease in the resistance.

## V. CONCLUSIONS

In conclusion, we have shown that the hysteresis in the temperature dependencies of magnetization and resistance in MnAs layers grown on GaAs(331) $B$  undergoes a permanent alteration until saturation is reached after few tens of thermal cycles around the phase-coexistence temperature range. In particular, the ferromagnetic phase is found to be stabilized, which is beneficial in spintronics applications. The alteration is evidenced to be a consequence of improvements in the material properties. The material modification is indicated to be driven by the out-of-plane components of the phase-transition stress resulting from the nonplanar geometry of the MnAs layer due to the step bunching in the GaAs buffer layer. We have shown that the stress is so large that massive plastic flow of materials takes place. The expansion of the hysteresis loops after thermal cycles suggests that the phase fractions in the layer change through nucleations in the phase domains rather than domain boundary movements.

The phenomenon demonstrates a dramatic influence of the substrate on a first-order phase transition in the overlayer. The present heterostructure thus presents an interesting system in which correlation between the physical properties and the structural properties can be systematically investigated. Moreover, it may provide an insight into the nature of the disappearance of the ferromagnetic order at  $T_C$ , which has been controversial.

## ACKNOWLEDGMENT

The authors wish to thank V. Kaganer for intriguing remarks.

<sup>1</sup>R. W. De Blois and D. S. Rodbell, Phys. Rev. **130**, 1347 (1963).  
<sup>2</sup>J. B. Goodenough and J. A. Kafalas, Phys. Rev. **157**, 389 (1967); N. Menyuk, J. A. Kafalas, K. Dwight, and J. B. Goodenough, *ibid.* **177**, 942 (1969).  
<sup>3</sup>M. K. Niranjan, B. R. Sahu, and L. Kleinman, Phys. Rev. B **70**, 180406(R) (2004).  
<sup>4</sup>H. Yamaguchi, A. K. Das, A. Ney, T. Hesjedal, C. Pampuch, D. M. Schaadt, and R. Koch, Europhys. Lett. **72**, 479 (2005).  
<sup>5</sup>R. H. Wilson and J. S. Kasper, Acta Crystallogr. **17**, 95 (1964).  
<sup>6</sup>C. Guillaud, J. Phys. Radium **12**, 223 (1951).  
<sup>7</sup>I. Rungger and S. Sanvito, Phys. Rev. B **74**, 024429 (2006).

<sup>8</sup>Y. Takagaki, L. Däweritz, and K. H. Ploog, Phys. Rev. B **75**, 035213 (2007).  
<sup>9</sup>K. Bärner, Phys. Status Solidi B **88**, 13 (1978).  
<sup>10</sup>M. Tanaka, Semicond. Sci. Technol. **17**, 327 (2002).  
<sup>11</sup>L. Däweritz, Rep. Prog. Phys. **69**, 2581 (2006).  
<sup>12</sup>M. Ramsteiner, H. Y. Hao, A. Kawaharazuka, H. J. Zhu, M. Kästner, R. Hey, L. Däweritz, H. T. Grahn, and K. H. Ploog, Phys. Rev. B **66**, 081304(R) (2002).  
<sup>13</sup>J. Stephens, J. Berezovsky, J. P. McGuire, L. J. Sham, A. C. Gossard, and D. D. Awschalom, Phys. Rev. Lett. **93**, 097602 (2004).

- <sup>14</sup>Y. Takagaki, C. Herrmann, J. Herfort, C. Hucho, and K.-J. Friedland, *Phys. Rev. B* **78**, 235207 (2008).
- <sup>15</sup>R. P. Panguluri, G. Tsoi, B. Nadgorny, S. H. Chun, N. Samarth, and I. I. Mazin, *Phys. Rev. B* **68**, 201307(R) (2003).
- <sup>16</sup>Y. Takagaki, C. Herrmann, B. Jenichen, J. Herfort, and O. Brandt, *Appl. Phys. Lett.* **92**, 101918 (2008); **92**, 179901 (2008).
- <sup>17</sup>V. H. Etgens, M. Eddrief, D. Demaille, Y. L. Zheng, and A. Ouerghi, *J. Cryst. Growth* **240**, 64 (2002).
- <sup>18</sup>D. K. Satapathy, V. M. Kaganer, B. Jenichen, W. Braun, L. Däweritz, and K. H. Ploog, *Phys. Rev. B* **72**, 155303 (2005).
- <sup>19</sup>V. M. Kaganer, B. Jenichen, F. Schippan, W. Braun, L. Däweritz, and K. H. Ploog, *Phys. Rev. Lett.* **85**, 341 (2000); *Phys. Rev. B* **66**, 045305 (2002).
- <sup>20</sup>T. Suzuki and H. Ido, *J. Phys. Soc. Jpn.* **51**, 3149 (1982).
- <sup>21</sup>H.-P. Schönherr, J. Fricke, Z. Niu, K.-J. Friedland, R. Nötzel, and K. H. Ploog, *Appl. Phys. Lett.* **72**, 566 (1998).
- <sup>22</sup>R. Nötzel and K. H. Ploog, *Jpn. J. Appl. Phys., Part 1* **39**, 4588 (2000).
- <sup>23</sup>Y. Takagaki, C. Herrmann, B. Jenichen, and O. Brandt, *Phys. Rev. B* **78**, 064115 (2008).
- <sup>24</sup>Y. Takagaki, E. Wiebicke, L. Däweritz, and K. H. Ploog, *Appl. Phys. Lett.* **85**, 1505 (2004).
- <sup>25</sup>G. Fischer and W. B. Pearson, *Can. J. Phys.* **36**, 1010 (1958).
- <sup>26</sup>S. Haneda, N. Kazama, Y. Yamaguchi, and H. Watanabe, *J. Phys. Soc. Jpn.* **42**, 1201 (1977).
- <sup>27</sup>K. Ryu, J. Kim, Y. Lee, H. Akinaga, T. Manago, R. Viswan, and S. Shin, *Appl. Phys. Lett.* **92**, 082503 (2008).